Electronic Supplementary Material (ESI) for Sustainable Energy & Fuels.
This journal is © The Royal Society of Chemistry 2019

Supplementary Information

Correlation between Ru-O Hybridization and Oxygen Evolution Reaction in Ruthenate Epitaxial Thin Films

Sang A Lee, [a,b*] *Jegon Lee,* [a*] *Seokjae Oh,* [a] *Suyoun Lee,* [c] *Jong-Seong Bae,* [d] *Won Chegal,* [e] *Mangesh S. Diware,* [f] *Sungkyun Park,* [g] *Seo Hyoung Chang,* [h] *Taekjib Choi,* [i] *Woo Seok Choi*[a**]

[a] Department of Physics, Sungkyunkwan University, Suwon 16419, Korea

[b] Department of Physics, Pukyong National University, Busan 48513, Korea

[c] Electronic Materials Research Center, Korea Institute of Science and Technology, Seoul 02792, Korea

[d] Busan Center, Korea Basic Science Institute, Busan 46742, Korea

[e] Advanced Instrumentation Institute, Korea Research Institute of Standards and Science, Daejeon 34113, Korea

[f] CeNSCMR and Department of Physics and Astronomy, Seoul National University, Seoul, 08826, Korea

[g] Department of Physics, Pusan National University, Busan 46241, Korea

[h] Department of Physics, Chung-Ang University, Seoul 06974, Korea

[i] Hybrid Materials Research Center, Department of Nanotechnology and Advanced Materials Engineering, Sejong University, Seoul 05006, Korea

Experimental details

Thin films growth and characterization. High-quality epitaxial CRO thin films were grown on atomically flat single-crystalline STO and Nb:STO substrates (CRO on Nb:STO was used for electrochemical experiments) via PLE at 700 °C. An excimer laser (248 nm, Lightmachinery, IPEX 864) with a fixed laser fluence of ~1.52 J/cm^2 and a repetition rate of 2 Hz was used. We systematically controlled the oxygen partial pressure from 0.1 to 100 mTorr during the film growth in order to modify the cation ratio in the thin films. All the thin films were structurally characterized using XRD (Rigaku, Smartlab & Pilatus (2D) detector).

Chemical stoichiometry. The chemical stoichiometry of the CRO thin films was studied at room temperature using an XPS system (Alpha+, Thermo Fisher Scientific, UK) with a monochromated Al-K_α X-ray source (hν = 1486.6 eV). The step size was 0.1 eV at a pass energy of 50.0 eV and 400 μm spot size. An NEC 6SDH pelletron accelerator with 3.0 MeV energy was used for RBS measurement. He^{+2} was used as the source gas and the tilting angle was set to 5°.

Optical properties. The optical properties of the CRO thin films were investigated using a highly surface sensitive tool, i.e., a spectroscopic ellipsometer (VUV-VASE Gen-II model, J. A. Woollam, Co., Inc.) at room temperature. The optical spectra were obtained at photon energies between 0.5 and 8.5 eV at an incident angle of 60°. A two-layer model (CRO thin film on STO

substrate) was sufficient for obtaining physically reasonable dielectric functions that reproduced the optical spectrum of CRO in the literature.

Electrochemical measurements. OER activity was measured using a potentiostat (Ivium Technologies) with a three-electrode set-up comprising a 3M NaCl saturated Ag/AgCl reference electrode, Pt mesh counter electrode, and high-quality epitaxial CRO thin film as the working electrode. The electrolyte (1.0 M KOH solutions) was prepared by mixing de-ionized water and KOH flakes (Sigma Aldrich). All polarization curves were obtained by sweeping from 0.2 to 1.7 V vs. a reversible hydrogen electrode (RHE) at a sweep rate of 10 mV s^{-1}. The sweep direction was set to the larger positive potential.

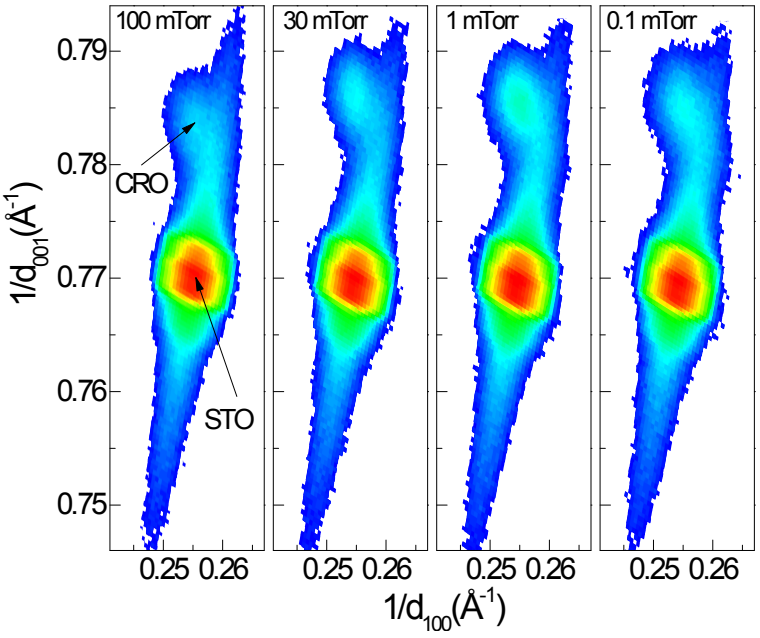

Figure S1. Reciprocal space maps of the $CaRuO_3$ thin films grown at $P(O_2)$ = 100, 30, 1, and 0.1 mTorr, near the (103) Bragg plane in the $SrTiO_3$ substrate.

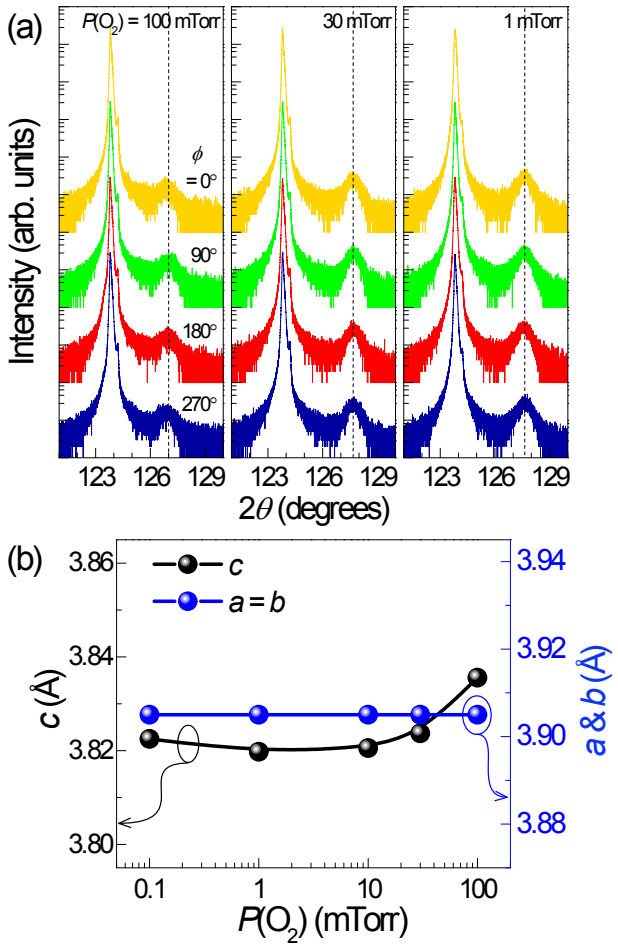

Figure S2. (a) Off-axis x-ray diffraction scans for the tetragonal $CaRuO_3$ thin films around (204) Bragg reflections from the $SrTiO_3$ substrate with φ = 0, 90, 180, and 270°. (b) Evolution of the lattice parameters as a function of $P(O_2)$.

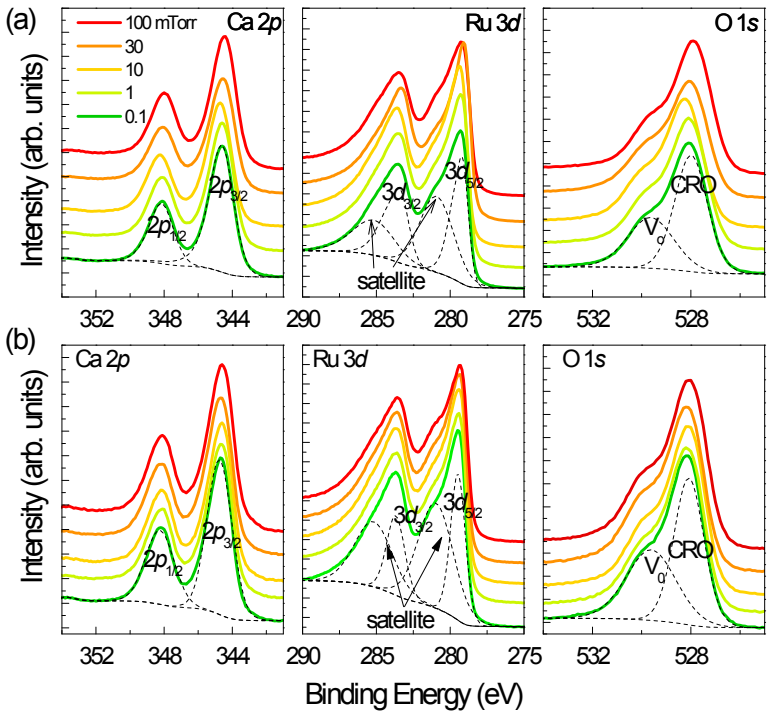

Figure S3. X-ray photoelectron spectroscopy for the Ca 2*p* core-level, Ru 3*d* core-level, and O 1*s* spectra for $CaRuO_3$ thin films grown at different $P(O_2)$ values (a) before and (b) after conducting cyclic voltammetry measurements, respectively. We could not find noticeable change in the thin film stoichiometry, even after the OER measurements.

$P(O_2)$ (mTorr)	Ca	Ru	O	Ca/Ru
100	1.03	0.93	3.04	1.11
10	0.99	1.02	2.99	0.97
1	1.12	0.88	2.93	1.37

Table S1. The atomic concentration determined from Rutherford backscattering spectroscopy.

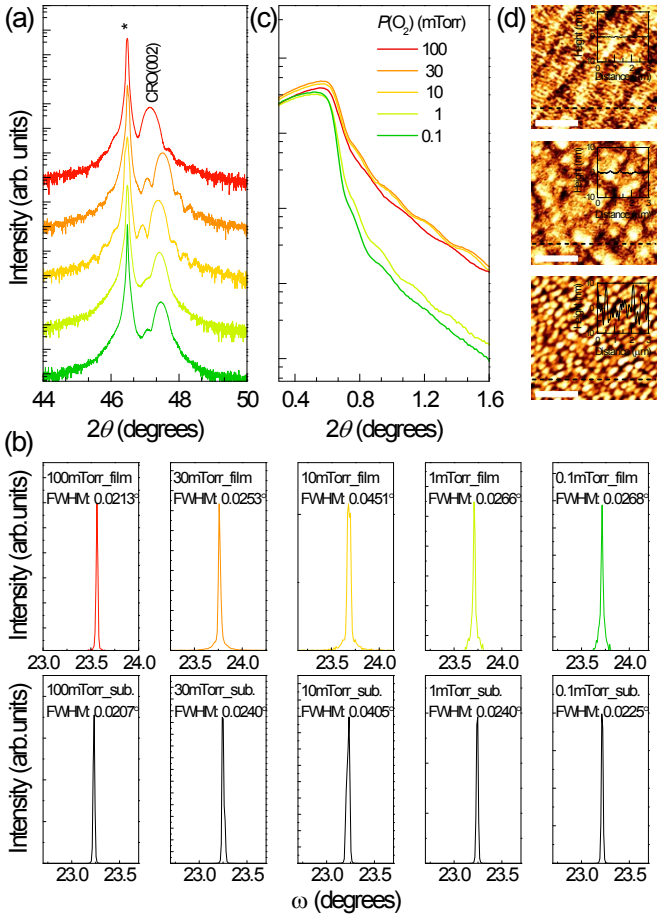

Figure S4. X-ray diffraction in epitaxial $CaRuO_3$ thin films grown on Nb:$SrTiO_3$ substrates with rocking curve measurements, showing the same crystalline quality as the thin films grown on $SrTiO_3$ substrates. Nb:$SrTiO_3$ substrates were employed as the bottom electrode for electrocatalytic measurements. (a) XRD θ-2θ scans for the epitaxially strained $CaRuO_3$ thin films grown at various $P(O_2)$ values around the (002) Bragg reflections from the $SrTiO_3$ substrates (denoted with *). Representative rocking curve measurements for the (002) Bragg refection from (b) the $CaRuO_3$ film with different $P(O_2)$ and the Nb-$SrTiO_3$ substrate. (c) XRR results show that

$CaRuO_3$ thin films with different $P(O_2)$ have thickness of ~30 ± 3 nm. (d) Topographic image and line scans of the $CaRuO_3$ films grown at 100, 10, and 0.1 mTorr. The scale bar is 3 μm.

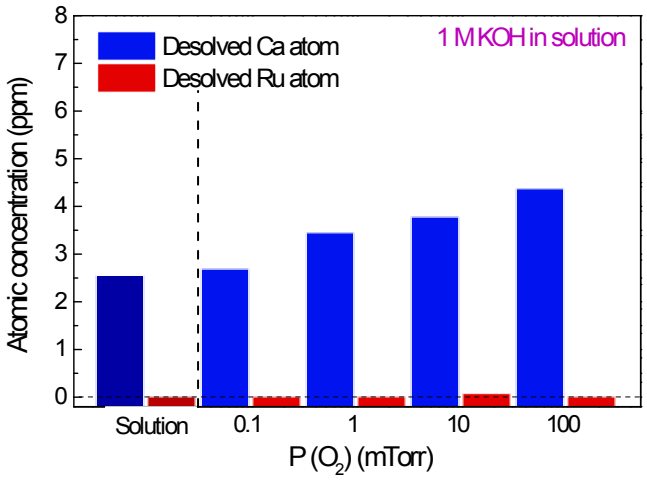

Figure S5. Atomic concentration of dissolved elements in the KOH solution after conducting cyclic voltammetry measurements obtained by inductively coupled plasma-optical emission spectrometry. The result indicates that the OER measurement does not strongly affect the concentration of dissolved species in the solution. In particular, no noticeable Ru dissolution was observed during the OER measurements.

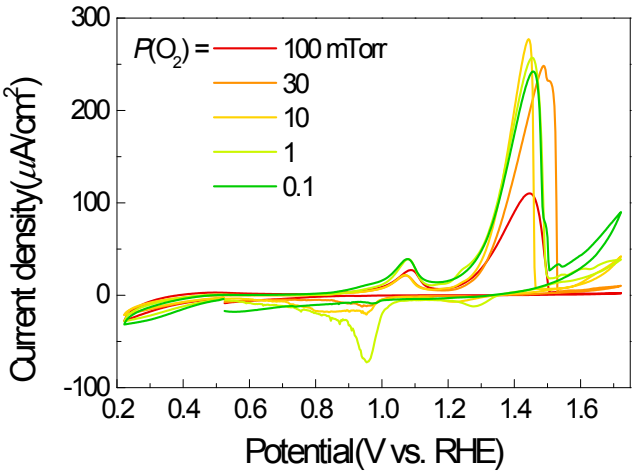

Figure S6. Cyclic voltammetry measurement for the $CaRuO_3$ thin films with various $P(O_2)$. The current densities are normalized by the geometric surface area. (Full scaled figure 4 (a))

$P(O_2)$ (mTorr)	RF (roughness factor)	Overpotential (V) @J (150 μA cm^{-2})	Specific current density (μA cm^{-2}) @η = 0.17 (V)	Tafel slope (mV decade^{-1})
100	1.000	-	90.76	174.26
30	1.000	0.183	132.19	122.46
10	1.001	0.147	203.20	120.24
1	1.070	0.150	188.54	158.37
0.1	1.073	0.156	175.74	162.70

Table S2. The surface roughness factor (RF), overpotential value at 150 μA/cm^2, specific current density at 0.17 V for overpotential, and Tafel slopes of epitaxial $CaRuO_3$ thin films grown at different $P(O_2)$.

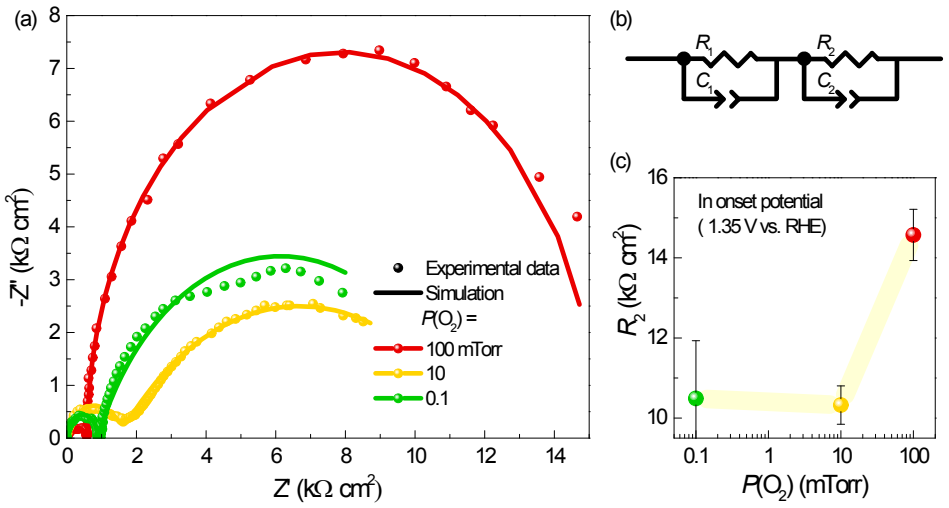

Figure S7. (a) Nyquist plot of electrochemical impedance spectra of the $CaRuO_3$ thin films with different $P(O_2)$. (b) Equivalent circuit in the impedance simulation and (c) the value of R_2 in equivalent circuit as a function of $P(O_2)$.

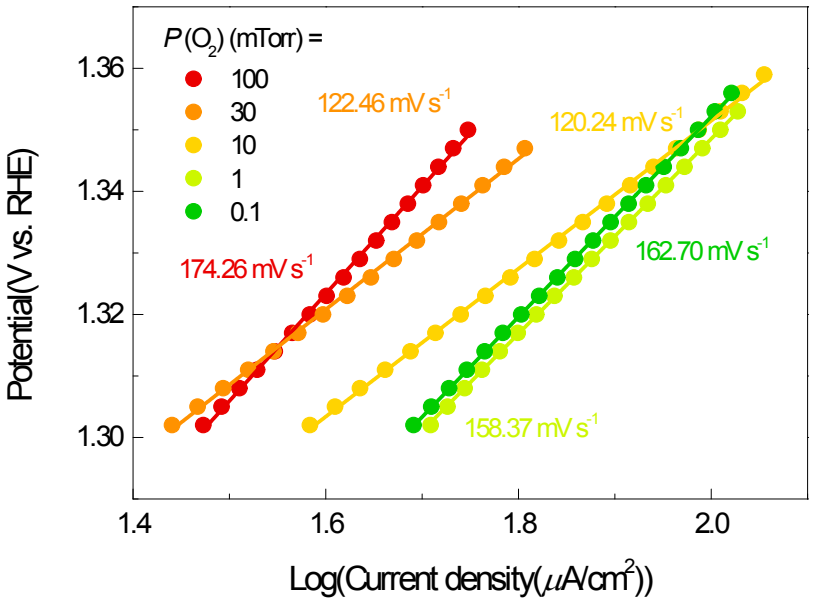

Figure S8. Tafel plots of epitaxial $CaRuO_3$ thin films grown at different $P(O_2)$ values. All the films are normalized to the catalyst surface area.

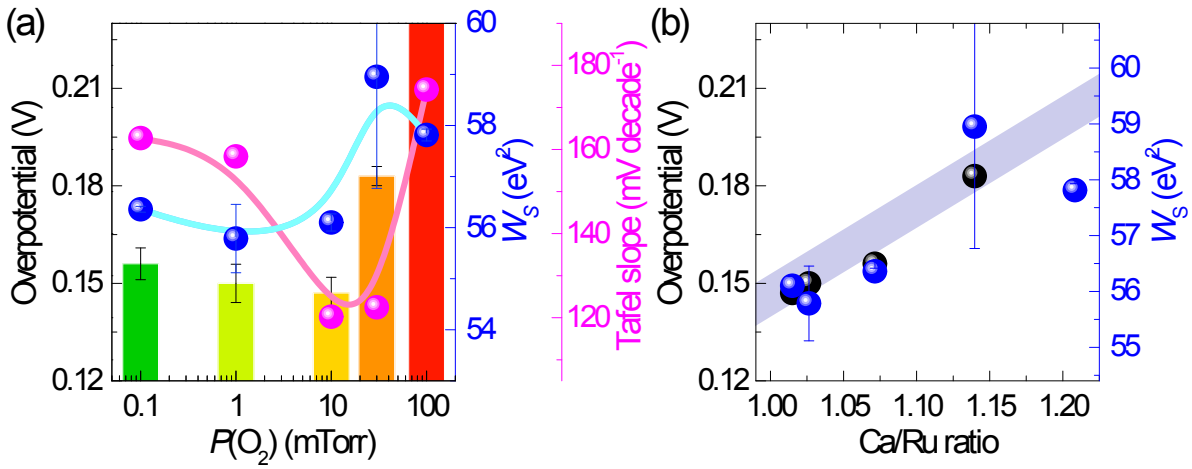

Figure S9. OER catalytic activity with modified electronic structure in $CaRuO_3$ thin films. (a) Overpotential around 100 μA/cm^2, Tafel slopes, and spectral weight of the $CaRuO_3$ thin film at the B peak as a function of $P(O_2)$. The OER activity shows the same trend as the charge transfer transition. (b) Overpotential and charge transfer transition for O $2p \rightarrow$ Ru $4d$ e_g as a function of the cation ratio. The relationship between overpotential and W_{sB} also show the same tendency, indicating that the OER activity is enhanced according to the decreased hybridization strength.